Conformational analysis of retinoids and restriction of their dynamics by retinoid-binding proteins

Daan M. F. van AALTEN*‡, Bert L. de GROOT†, Herman J. C. BERENDSEN† and John B. C. FINDLAY*

*Department of Biochemistry and Molecular Biology, University of Leeds, Leeds LS2 9JT, U.K., and †Groningen Biomolecular Sciences and Biotechnology Institute (GBB), Department of Biophysical Chemistry, the University of Groningen, Nijenborgh 4, 9747 AG Groningen, The Netherlands

An exhaustive sampling of the configurational space of all-*trans* retinol using a 0.1 μs molecular-dynamics simulation is presented. The essential dynamics technique is used to describe the conformational changes in retinol using only three degrees of freedom. The different conformational states of retinol are analysed, and differences in free energy are calculated. The essential dynamics description allows a detailed comparison of free retinol and retinoids bound to retinoid-binding proteins and opens new possibilities in the small-molecule docking field. The dynamics of retinoids when complexed with their binding proteins are restricted, and they are forced into strained conformations. A 'spring' model for retinoid binding is proposed. This model is extended to a hypothesis for retinoid binding to visual pigments and bacteriorhodopsin.

INTRODUCTION

Retinoids are involved in a variety of important biological processes. In the retina, retinal is bound to opsin, forming rhodopsin (Rho), a complex able to convert the energy of a photon into activation of neural cells. Similarly, bacteriorhodopsin (bR) acts as a proton pump, converting light energy to a proton gradient via its bound chromophore, retinal. The role of retinal in these two processes is crucial. The absorbed photon initiates rotation around a double bond in the polyene tail of the ligand, which in turn brings about a conformational change in the protein. Although low-resolution structures are available for Rho and bR [1–3], they do not provide sufficient detail for a study of retinal conformation, let alone retinal dynamics. NMR studies into the conformation of retinal bound to bR/Rho have provided additional detail, especially concerning the position of the methyl groups and the conformation of the β-ionone ring [4–6].

Here we address the question: what could happen to the structure and dynamics of retinal when it binds to bR and Rho as compared with free retinal in solution. Since no high-resolution structure is available for retinal bound to bR/Rho, we have used an alternative approach to this problem. Instead of studying free retinal and retinal in bR/Rho, we examined free retinol and retinoids liganded to retinoid-binding proteins for which several high-resolution structures are available. The observations were then extrapolated to generate a hypothesis concerning the retinal conformational changes in bR/Rho, providing support for the spectral tuning 'strain' model [7]. The new technique of 'essential dynamics' (ED) [8] was used to extract collective degrees of freedom from a molecular dynamics (MD) simulation of free retinol. Comparison reveals that retinoid structure in some binding proteins is strained and that its dynamics are restricted.

METHODS

The ED method [8] is able to extract the large concerted motions of atoms from an MD trajectory produced with a standard MD program. The first step involves the construction of a covariance matrix:

$$C_{ij} = \langle (x_i - x_{i,0})(x_j - x_{j,0}) \rangle \tag{1}$$

where $x_{i,j}$ are separate x, y, z coordinates of the atoms, x_0 is the average position of the coordinates and the average is calculated over the whole trajectory, after all frames were fitted on a reference structure to remove overall translational and rotational motion. This covariance matrix is then diagonalized, yielding a set of eigenvalues and eigenvectors. The eigenvectors indicate directions in a $3n$-dimensional space (with n = number of atoms), that is, concerted fluctuations of atoms. The eigenvalues are equivalent to the total mean square displacement of atoms along their corresponding eigenvectors. In the case of proteins, there are always only a few eigenvectors with large eigenvalues, so the large overall motion of the protein can be adequately described using only a few eigenvectors [8–11].

In a previous paper dealing with extending the sampling of the configurational space of proteins [12], the following procedure was proposed: the positions along a few essential eigenvectors (typically the first three) are constrained during MD in such a way that the accessible space is sampled at an enhanced rate, compared with usual MD. When a complete enough sampling is reached, it becomes meaningful to analyse certain physical properties over a grid in the essential subspace. In this way, the dependence of this physical property (e.g. energy or hydrogen bonding and secondary structure in case of proteins) on the position in the essential subspace can be evaluated. Here, we produced a very long free MD run of retinol; at every step of the simulation the projection of the structure on certain eigenvectors was calculated, and the structure was assigned to a grid point by dividing the projections by a certain interval (here a grid size of 0.03 nm is used). Physical properties are then calculated from the structure and 'stored' at that grid point. At the end of the simulation the average physical property is calculated at each grid point. This approach is only possible if a sufficiently large sampling has been produced, which, as will be shown later,

appears to be the case for retinol. Two properties were investigated: the average potential energy and the density, i.e. how often each grid point is visited during the simulation. The results of the simulation of free retinol were then compared with an MD simulation of retinol bound to the cellular retinol-binding protein, type I (cRBP), and to structures of retinoids found in the crystal structures of retinoid-binding proteins.

All energy minimizations (EM) and MD runs were performed using the GROMOS program suite [13]. The simulation of free retinol was started from the all-*trans* conformation found in the crystal structure of cRBP [14]. GROMOS uses a united atom approach, i.e. methyl groups are modelled by a single atom with an increased van der Waals radius. Only the polar retinol hydroxyl hydrogen was taken into account explicitly. The topology for retinol was that taken from the 'RTOL' entry in the RT37C.DAT GROMOS topology building-block file. The structure was energy minimized using the conjugate gradients algorithm with no non-bonded forces cutoff. SHAKE [15] was used to restrain bonds to their equilibrium lengths, allowing a simulation time step of 2 fs. The simulation was performed *in vacuo* to represent an apolar solvent and allow exhaustive sampling. An MD startup run of 25 ps was performed using velocities taken from a Maxwellian distribution at 300 K. The MD run was then continued for 0.1 μs using coupling to an external heat bath [16] with a coupling constant of 0.1 ps.

A previously published 300 ps full solvent MD run of retinol bound to cRBP was used for comparison with the free retinol simulations [10]. Visual inspection of structures was done with WHAT IF [17].

RESULTS

MD of retinol

In order to validate our MD simulation of retinol, several physical properties that can be linked directly to experimental data were calculated. One of the most interesting properties of retinol is the rotation around the C6–C7 bond (Figure 1), that is, the orientation of the ring with respect to the polyene tail. X-ray crystallographic, NMR and theoretical studies of retinoids have shown that the most frequently occurring orientation is *S-cis* (i.e. pseudo-*cis* because it is a single, not a double bond) with angles of ± 35–80 degrees [18–21]. The rotation around the C6–C7 bond during the MD simulation is shown in Figure 2 (top). There are two stable interconverting conformations, -70 and $+70$ degrees, in agreement with the experimental results, with an average lifetime of approximately 1.0 ns.
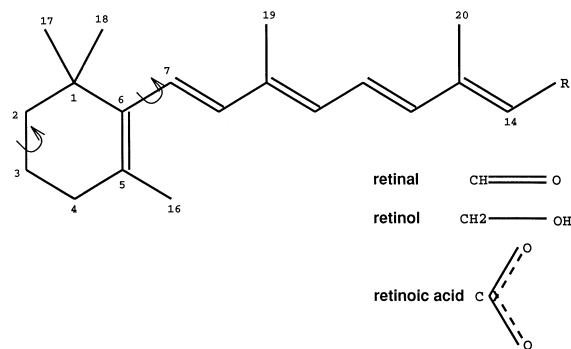

Figure 1   Structure of all-*trans* retinoids

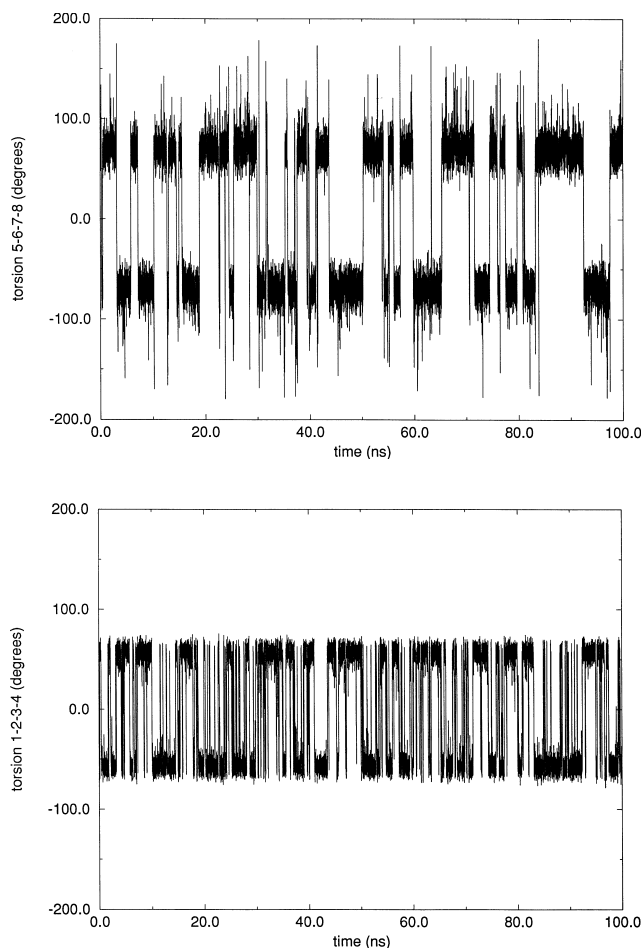Curly arrows indicate torsion angles discussed in the text.

Figure 2   Torsion angles C5–C6–C7–C8 (top) and C1–C2–C3–C4 (bottom) as a function of simulation time

The retinol ring is based on a cyclohexene skeleton. Cyclohexene has been shown to exist in two main conformations [22,23]. In both, the atoms equivalent to C1, C4, C5 and C6 lie in one plane. Either the C2 or the C3 atom (which both lie opposite the double bond in the ring; see Figure 1) lies above the plane, the other below. The C1–C2–C3–C4 torsion angle has been shown to be either -57 or $+57$ degrees [22,23]. The two states rapidly interconvert with a conformer life time in the order of 1 ns, measured by NMR [22]. The rotation around the C2–C3 bond during the MD simulation is shown in Figure 2 (bottom). There are two stable conformations at -57 and $+57$ degrees. The average conformer life time is 0.32 ns. Both rotation angle and conformer life time are in agreement with the experimental results [22,23].

In short, physical properties derived from the MD simulation are in agreement with experimental results. This indicates that, based on the (limited) experimental data, the simulation seems to be reliable, even though it was performed *in vacuo* with a classical approach. Therefore, this simulation can subsequently be used for ED analysis.

ED analysis of retinol

The first 20 atoms (C1–C20) of retinol [i.e. excluding the terminal hydroxy group (Figure 1), chosen to facilitate comparison] were used to construct a covariance matrix that was subsequently
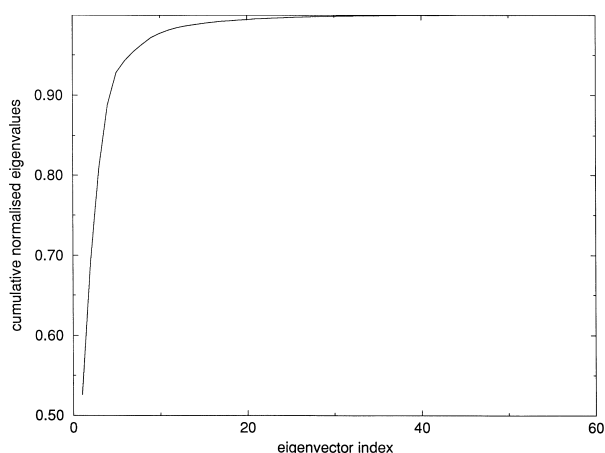
Figure 3 Cumulative normalized eigenvalues

For each eigenvector the relative contribution to the total motion of the molecule is calculated and then added to these values of the previous eigenvectors. This shows that we only need the first few eigenvectors to describe 90% of the motion of the molecule.
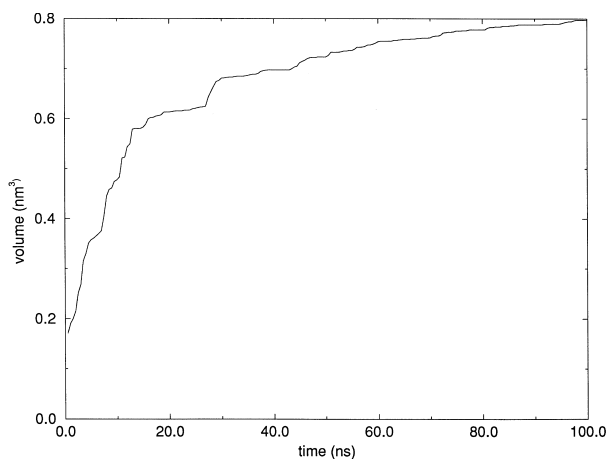

Figure 4 Sampled volume in the essential subspace spanned by the first three eigenvectors as a function of simulation time

diagonalized as described previously [8]. The cumulative normalized eigenvalue curve (Figure 3), which reveals the summed contribution of all individual eigenvectors to the total fluctuation of the molecule, shows that the first three eigenvectors describe approx. 80% of the total fluctuation. Thus, almost all conformational states of retinol can be described by a three-dimensional (3D) 'essential subspace'.

We aimed at obtaining a fully sampled configurational space of retinol by the 0.1 μs MD simulation. The total sampled volume in the 3D essential subspace as a function of time was calculated using a method described elsewhere [24]. In short, this involves (in the case of three eigenvectors) making a small cubic grid in the essential subspace and then counting how many of these cubes are visited during the simulation as a function of time. If this number is increasing, this would mean that the simulation is still visiting new areas of the essential subspace. Figure 4 shows that, after 0.1 μs, the essential subspace spanned by the first three eigenvectors is almost fully sampled, as judged by the levelling off of the curve.

The motions found in the essential subspace are depicted in Figure 5. Eigenvectors 1 and 2 together describe the rotation of the ring and tail with respect to each other, with eigenvector 1 showing mainly the rotation of the tail, and eigenvector 2 the rotation and bending of the tail. Since the covariance matrix is constructed from atomic displacements in Cartesian space, it is to be expected that a large rotational motion of a group of atoms cannot be described by a single eigenvector. Probably the first two eigenvectors need to be taken together to accurately describe the rotation of the ring and tail with respect to one another. Eigenvector 3 shows the ring inversion as described above, the two atoms opposite the double bond in the β-ionone ring taking up two different conformations.

Thus, it seems that the ED technique is able to describe the conformational changes in retinoids with only three eigenvectors, compared with the initial 60 degrees of freedom. A similar reduction in degrees of freedom has been found for proteins [8–10]. Hence ED, so far only applied to large systems like proteins, is also applicable to small molecules like retinoids. Since the configurational space appears to be sampled completely, properties in the essential subspace spanned by the first three eigenvectors can now be examined.

Properties in the essential subspace

To enable a detailed comparison of the structural and dynamic properties of the simulation of free retinol and retinoids bound to proteins, energetically favourable and unfavourable states and the energy differences between them need to be defined. Properties were investigated as a function of the displacement along a single eigenvector, of the position in a plane spanned by a combination of eigenvectors 1, 2 and 3, and of the position in a 3D space spanned by these eigenvectors. The 3D density (i.e. how often each grid point is visited during the simulation; see the Methods section) profile is shown in Figure 6 (left panel). The density and average total potential energy in the 1–2, 1–3 and 2–3 eigenvector planes are shown in Figure 6, the middle and right panels respectively. Several observations can be made from these plots.

(i) The properties show a kind of symmetry along eigenvectors 1 and 3. This is expected, since the motions along these eigenvectors (see Figure 5) are also symmetrical. This is further evidence that the space is well sampled.

(ii) The essential subspace shows two dominating conformations, each linked to another less favoured conformation, especially well depicted in the 3D plot (Figure 6, left panel) as connected patches of high density. In essence, these represent the two *S-cis* low-energy conformations around the C6–C7 bond (Figures 1 and 5) together with the ring inversion. As can be seen from the 1–3 plots, for each conformer along eigenvector 1 there are two possible conformations along eigenvector 3, of which one is favoured. There appears to be a significant degree of coupling between these eigenvectors. When eigenvector 1 has a negative projection (i.e. is in one of the two possible conformations around the C6–C7 bond), the conformation that has a positive projection along eigenvector 3 is favoured; it is the other way round for the positive projection along eigenvector 1. Hence ring rotation and ring inversion are coupled. The two favoured conformations are shown in Figure 7.

(iii) There is a high degree of correlation between the density distribution and the total potential energy. Areas with a high density also have a low average total potential energy. The energy plots, however, contain a higher amount of noise, probably indicating that there may be significant contributions from conformational changes described by other eigenvectors.

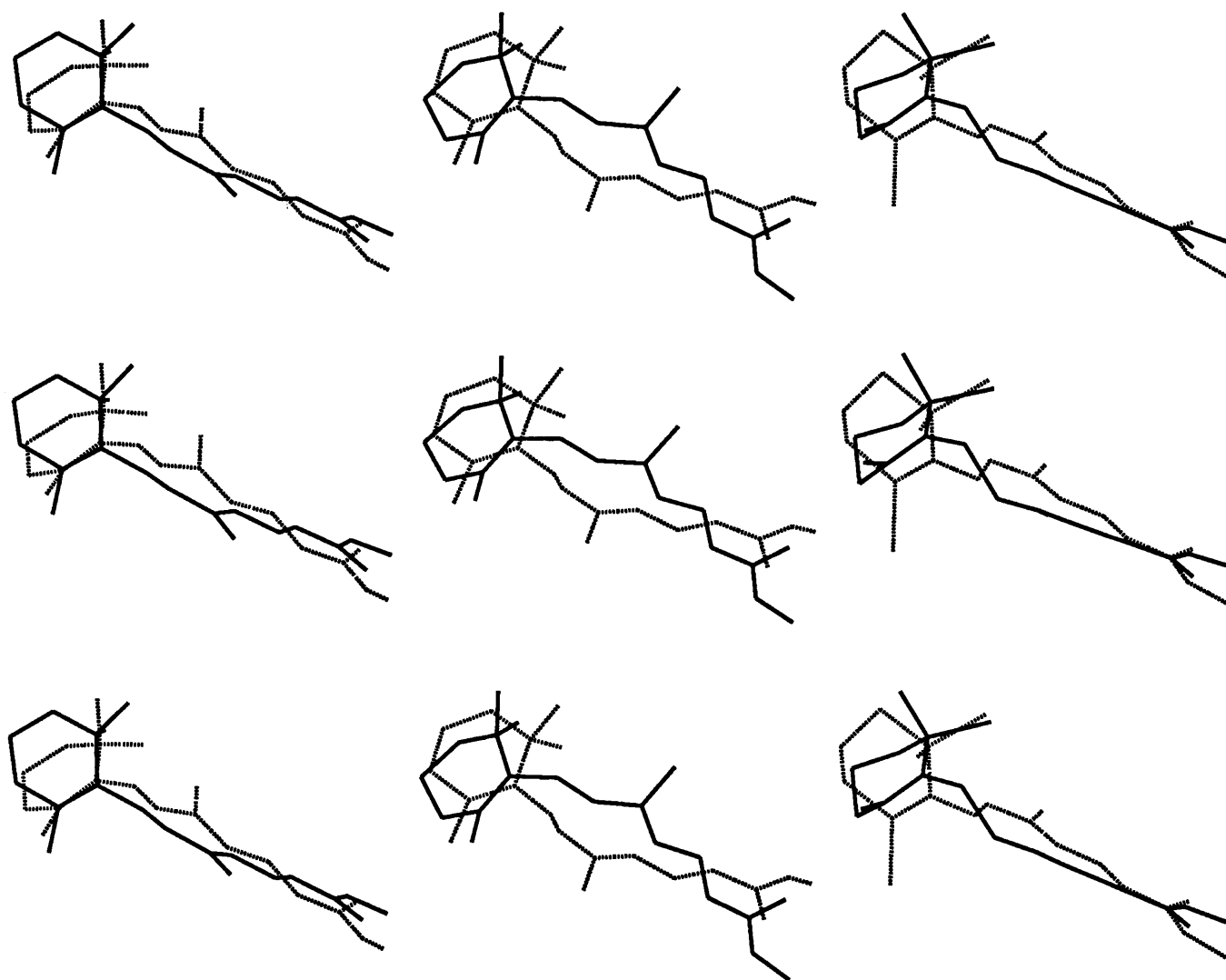Since we have fully sampled the retinol configurational space

Figure 5   Examples of the structures along eigenvector 1 (left panel), 2 (middle panel) and 3 (right panel)

Three-centred stereo pictures (i.e. use a pair of stereo glasses to view the left two pictures of each panel using cross-eyed stereo or the right two pictures using diverged stereo), by arbitrarily projecting them at −0.3 (dotted line) and +0.3 nm (solid line) with respect to the average.

and have approximated an apolar solvent by simulating retinol *in vacuo*, we can estimate differences in free energy (or potential of mean force with respect to an essential coordinate) directly by:

$$\Delta A_i = -\text{R}T\ln(\rho_i/\rho_0) \tag{2}$$

where ΔA_i is the free-energy difference between state i and a chosen reference, R is the gas constant, T is temperature and ρ is the density. Using

$$\Delta A = \Delta U + T\Delta S \tag{3}$$

where S is entropy, it is possible to estimate the entropy contribution, since ΔU is delivered by calculating the average total potential energy. ΔA and ΔU as functions of the displacement along eigenvector 1 are shown in Figure 8. The ΔA and ΔU curves have a high degree of overlap, indicating that the free-energy landscape is dominated by the energy contribution and

that entropy plays only a minor role. As estimated from the ΔA curve, rotating from one *S-cis* conformation to the other (see Figure 7) costs about 2 kcal/mol.

Comparison with retinoids bound to proteins

We now turn to the investigation of retinoid conformation in proteins. The PDB database [25] was scanned, and two different types of all-*trans* retinoid-binding protein were isolated.

Plasma retinol-binding proteins

Structures used from this family contained retinol (1BRP [26], 1HBP [27] and 1RBP [28]) or retinoic acid (1FEM [29]).

Cellular retinol-binding proteins

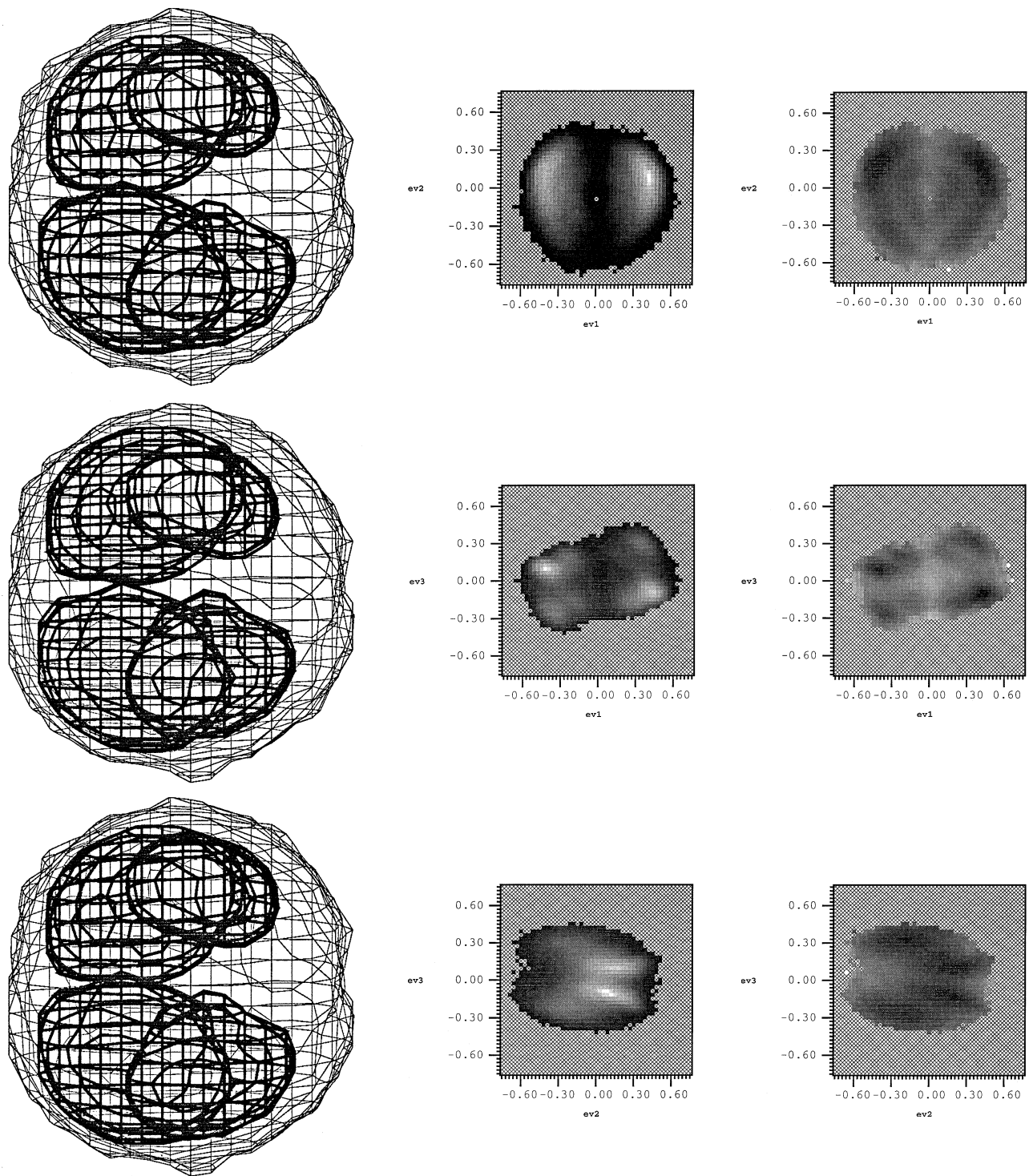This set of structures contained three different retinoids: retinol

Figure 6 Profiles of eigenvector planes

Left: Three-centred stereo picture (see the legend to Figure 5) of the 3D iso-density profile viewed on to the eigenvector 1–2 planes. The outer shell (thin line) represents the edges of the sampled space, i.e. grid points that are visited once or more. The inner shell (bold line) contains all points that are visited at least 15 times. Middle: Two-dimensional density profiles in the (from top to bottom) 1–2, 1–3 and 2–3 eigenvector planes. Black represents the lowest density, white the highest, and values in between are scaled using a linear greyscale. Right: Average total potential energy as a function of the position in the eigenvector planes 1–2, 1–3 and 2–3 (from top to bottom). Black represents the lowest energy, white the highest energy, and values in between are scaled using a linear grey scale. ev1, ev2 and ev3 are eigenvectors 1, 2 and 3 respectively.
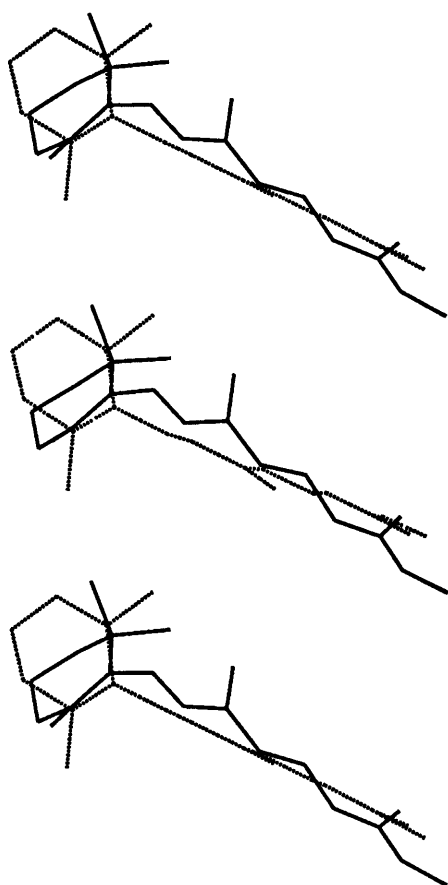
Figure 7 Conformations at the two highest density points in the 3D essential space

Three-centred stereo picture (see the legend to Figure 5), at approximately $(-0.45, 0.1, 0.1)$ (dotted line) and $(0.45, 0.1, -0.1)$ (bold line).

Figure 8 ΔA (Helmholtz free-energy difference) and ΔU (average total potential energy difference) as functions of displacement along eigenvector 1

(1CRB [14]), retinal (1OPB [30]) and retinoic acid (1CBR [31], 1CBS [31]).

The common retinoid cores (the C1–C20 atoms) were extracted, fitted on to the same reference structure as was used for the simulation of free retinol, and projected on to the free retinol eigenvectors (Figure 9). The retinoids in the plasma retinoid-binding proteins all seem to cluster in a region of the essential subspace that is favoured by the simulation of free retinol (Figure 6, middle panel). With cellular retinol-binding proteins, however, a different behaviour is observed. The retinoids are not clustered in a single region of the essential subspace. However, comparison with Figure 6 (middle panel) reveals a common feature: the retinoids in this type of binding protein are stressed into higher energy conformations. Based on estimates from free-energy calculations, these conformations are about 1 kcal/mol higher in free energy than the ground state. These retinoid-binding proteins have a retinoid-binding pocket lined with hydrophobic residues; hence this cost in energy is easily compensated by the hydrophobic effect [32,33]: shielding both the hydrophobic pocket and retinol from the polar solvent. But what would be the point of binding retinol in an unfavourable conformation if it is in principle possible to bind it in the ground state, as demonstrated by the group of plasma retinol-binding proteins? This problem was studied by analysing the conforma-
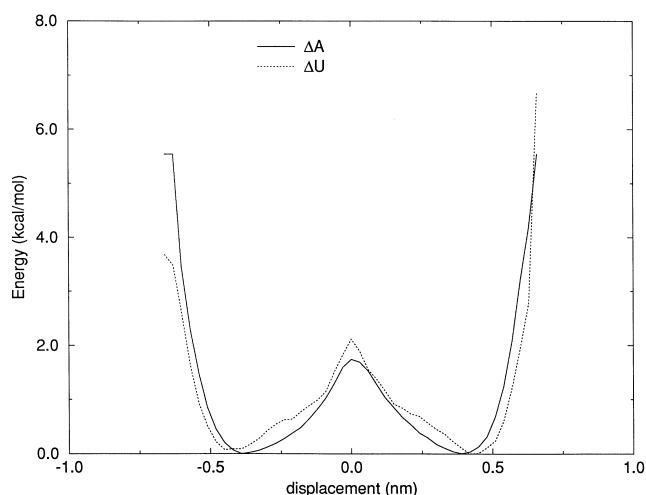
tional changes in retinol during an MD simulation of a cellular retinoid-binding protein.

Dynamics of retinol bound to the cellular retinol-binding protein

A previously published 300 ps trajectory of the cellular retinol-binding protein [10] was used to analyse protein-bound retinol dynamics. Retinol coordinates were extracted from the normal MD trajectory and also from the second eigenvector trajectory for the protein and retinol together (see [10]) to reveal the correlation of large concerted motions in the protein and the ligand. The resulting retinol trajectories were projected on to the eigenvectors from the simulation of free retinol (Figure 10). There are some significant motions in the configurational space of retinol caused by the protein. During the MD simulation of the protein, retinol is markedly pushed along eigenvector 2 of free retinol; i.e. retinol acts like a spring, wound by the protein. Presumably, when retinol exits the protein, it 'unwinds' to the stable *S-cis* conformation observed in solvent (see Figure 7).

DISCUSSION

The physical properties derived from the simulation of free retinol suggest that the structure and dynamics of retinol are well modelled using the GROMOS forcefield, even though the simulation was performed *in vacuo* and the forcefield is based on classical mechanics and uses the 'united atom' approach [13]. The rotational conformers around the C6–C7 bond are well reproduced, as are the parameters connected to the cyclohexene ring inversion. Various theoretical studies towards retinoid conformation have been published [20,23,34–36]. In most of them, a quantum mechanical approach was used. All found the *S-cis* conformer to be the stable conformation of free retinoid. Calculated energy barriers for rotation of one *S-cis* conformer to the other ranged from 4 to 8 kcal/mol. Here, we find a value of only 2 kcal/mol. However, most calculations assumed a fixed ring and a fixed tail. When the crystal structures [18,19] and the results presented here are investigated this appears not to be a valid approximation. The tail is bent with respect to the ring, and strain is further relieved by ring puckering. Thus, it seems that our simulation model for retinol reproduced experimental and
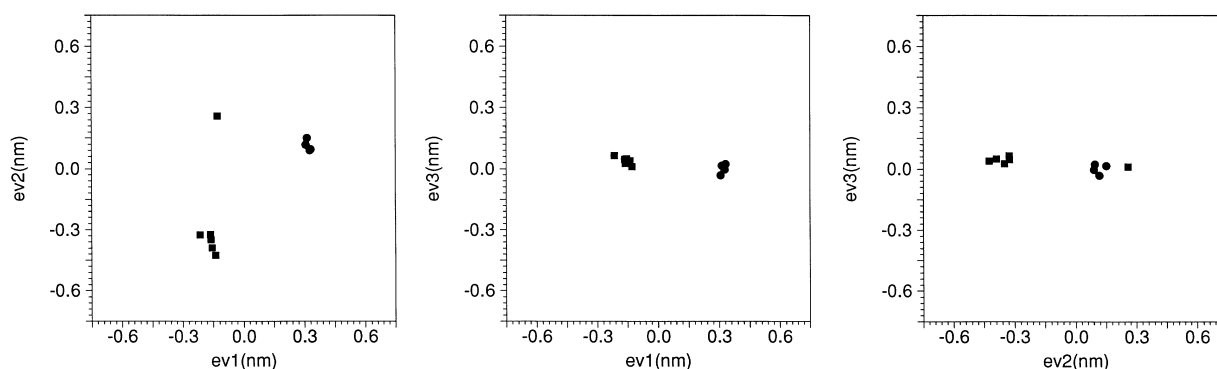
Figure 9   Projections of retinoid structures found in protein crystal structures on to the 1–2, 1–3 and 2–3 (from left to right) eigenvector planes

Circles are retinoids in plasma retinoid-binding proteins; squares are retinoids in cellular retinoid-binding proteins. ev1, ev2 and ev3 are eigenvectors 1, 2 and 3 respectively.
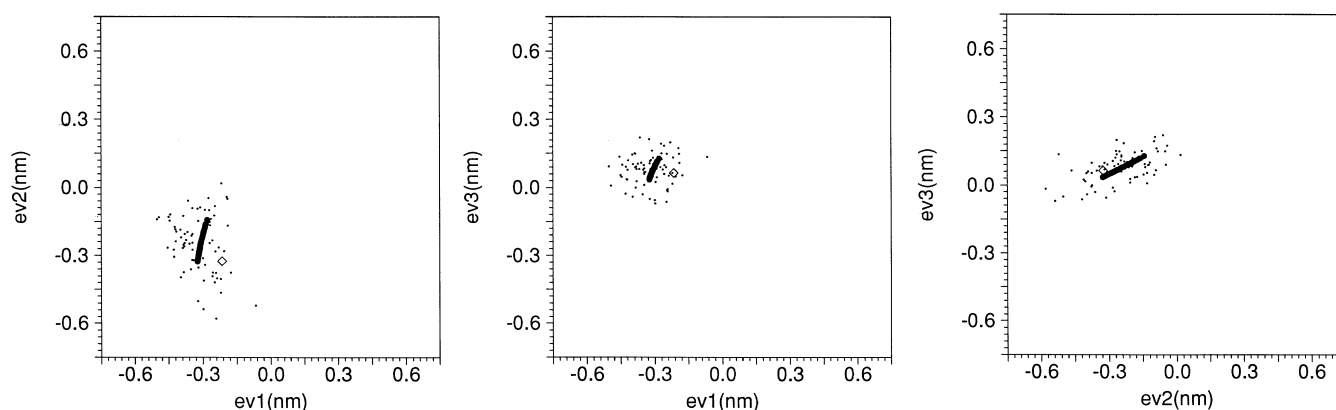

Figure 10   Projections of the retinol structures from a free MD simulation (small dots), the second eigenvector from this MD simulation (bold line) and the cRBP crystal structure [14] (open diamond) on to the 1–2, 1–3 and 2–3 eigenvector planes from the free retinol simulation

ev1, ev2 and ev3 are eigenvectors 1, 2 and 3 respectively.

theoretical values and can be reliably used in simulation of retinoid–protein complexes, as shown before for both plasma and cellular retinol-binding proteins [10,37]. Although the use of the GROMOS thermostat [16] might not be appropriate for such a small molecule, it does seem to lead to properties that are in agreement with experimental data. We have repeated the simulation with a very tight coupling (2 fs, the same as the time step), and although this did change the differences in free energies, the overall picture of conformations was not changed.

The ED analysis proved to be useful in describing retinoid dynamics; a 3D essential subspace could be derived that contained 80% of the total motion of the free retinol simulation. Ring and tail motions as well as ring inversion and the correlations between them were described. Analysis of the essential subspace identified low-energy conformers and enabled quantitative approximation of the free-energy differences between them. The energy differences between the conformers could also have been analysed by normal modes [38]. ED, however, can be performed without any knowledge about any preferred conformations beforehand, whereas a normal modes analysis would heavily depend on a chosen structure. Normal modes analysis studies structures in a local minimum, whereas our ED analysis is able to describe conformational changes that cover several such minima, free of bias.

Retinol seems to be bound to cRBP in a strained conformation. UV/visual spectral analysis has shown that there is a significant red shift (about 25 nm) of the retinoid absorbance peak when retinoids bind to the cellular retinol-binding protein [39–42]. Studies of model compounds have shown that this shift indicates that the ring is in the strained *S-trans* conformation with respect to the tail [43,44]. Motion along the essential coordinates of retinol was observed when the protein was simulated [10]. Retinol may act like a spring, forced in the strained *S-trans* conformation, possibly facilitating retinol to transfer from the binding pocket of cRBP to that of another protein. This correlates with the function of cRBP, which acts as a simple carrier protein, transporting retinol from one protein to the other [45,46].

As mentioned in the Introduction, retinoids play a role in the visual cycle, being the first step in the transduction of light energy to nerve signals (in the visual pigment Rho) or the conversion of light to a proton gradient (in bR). When retinal, the chromophore in both bR and Rho, binds to the protein, a large bathochromic shift is observed [47]. This bathochromic shift has been explained using two models:

The strain model

Changing the orientation of the ring with respect to the tail

changes the amount of conjugation and hence the spectrum of the retinoid [7,43,44,48].

The charge model

The spectrum is changed by protonating the Schiff's-base linkage of the retinoid to the protein and by further interaction of the retinoid with charged residues in the binding site [7,49–52].

The dominating contribution to the bathochromic shift is thought to be provided by the charge effect. However, it has been shown that retinol, which cannot form a Schiff's-base linkage, binds to bR also with a bathochromic shift [47]. There may be some contribution of the strain model when retinoids bind to bR. Retinal has been shown to adopt the highly strained *S-trans* conformation in the dark-adapted state of bR [53]. Possibly, this strain plays a similar role to that found for the cellular retinoid-binding protein, where conformational changes in the retinoid were linked to the dynamics of the protein. Retinal is bound to bR in a strained conformation and with restricted dynamics. Instead of releasing this stress energy by dissociating from the protein, the energy is released after extra energy has been added in the form of a photon, providing the activation energy for a rotation around a double bond, thus releasing the spring and causing a conformational change in the protein. A similar sequence of events may play a role in visual rhodopsins.

Finally, it is expected that the results presented here may lead to new developments in receptor–ligand docking algorithms. It appears we are now able to express both proteins and small molecules in terms of a few degrees of freedom. As suggested before [54], a protein might be simulated using an algorithm that artificially speeds up the essential motions, increasing the chance of a ligand entering the binding site . First steps in this direction have already been taken for proteins [12,24]. Now, using the results presented here, this approach may be extended to (flexible ligand)–(flexible receptor) algorithms.

REFERENCES

1   Henderson, R., Baldwin, J. M., Ceska, T. A., Zemlin, F., Beckmann, E. and Downing, K. H. (1990) J. Mol. Biol. **213**, 899–929
2   Schertler, G. F. X., Villa, C. and Henderson, R. (1993) Nature (London) **362**, 770–772
3   Unger, V. M. and Schertler, G. F. X. (1995) Biophys. J. **68**, 5370–5375
4   Ulrich, A. S., Heyn, M. P. and Watts, A. (1992) Biochemistry **31**, 10390–10399
5   Ulrich, A. S., Watts, A., Wallat, I. and Heyn, M. P. (1994) Biochemistry **33**, 5370–5375
6   Ulrich, A. S., Wallat, I., Heyn, M. P. and Watts, A. (1995) Nat. Struct. Biol. **2**, 190–192
7   Honig, B., Greenberg, A. D., Dinur, U. and Ebrey, T. G. (1976) **15**, 4593–4599
8   Amadei, A., Linssen, A. B. M. and Berendsen, H. J. C. (1993) Proteins **17**, 412–425
9   van Aalten, D. M. F., Amadei, A., Vriend, G., Linssen, A. B. M., Venema, G., Berendsen, H. J. C. and Eijsink, V. G. H. (1995) Proteins **22**, 45–54
10   van Aalten, D. M. F., Findlay, J. B. C., Amadei, A. and Berendsen, H. J. C. (1996) Prot. Eng. **8**, 1129–1135
11   van Aalten, D. M. F., Amadei A., Bywater, R., Findlay, J. B. C., Berendsen, H. J. C., Sander, C. and Stouten, P. F. W. (1996) Biophys. J. **70**, 684–692
12   Amadei, A., Linssen, A. B. M., de Groot, B. L., van Aalten, D. M. F. and Berendsen, H. J. C. (1996) J. Biomol. Struct. Dyn. **13**, 615–625
13   van Gunsteren, W F. and Berendsen, H. J. C. (1987) Gromos manual. BIOMOS, Biomolecular Software, Laboratory of Physical Chemistry, University of Gröningen, The Netherlands
14   Cowan, C. W., Newcomer, M. E. and Jones, T. A. (1993) J. Mol. Biol. **230**, 442–446
15   Ryckaert, J. P., Ciccotti, G. and Berendsen, H. J. C. (1977) J. Comp. Phys. **23**, 327–341
16   Berendsen, H. J. C., Postma, J. P. M., DiNola, A. and Haak, J. R. (1984) J. Chem. Phys. **81**, 3684–3690
17   Vriend, G. (1990) J. Mol. Graph. **8**, 52–56
18   Hamanaka, T. and Mitsui, T. (1972) Acta. Crystallogr **b28**, 214–222
19   Gilardi, R., Karle, I. K., Karle, J. and Sperling, W. (1971) Nature (London) **232**, 187–189
20   Honig, B., Hudson, B., Sykes, B. D. and Karplus, M. (1971) Proc. Nat. Acad. Sci. U.S.A. **68**, 1289–1293
21   Ippel, J. H., Spijker-Assing, M. B., Groesbeek, M., van der Steen, R., Altona, R. and Lugtenburg, J. (1994) Recl. Trav. Chim. Pays-Bas **113**, 99–108
22   Anet, F. A. L. and Haq, M. Z. (1965) J. Am. Chem. Soc. **87**, 3147–3150
23   Saebo, S. and Boggs, J. E. (1981) J. Mol. Struct. **73**, 137–144
24   de Groot, B. L., Amadei, A., van Aalten, D. M. F. and Berendsen, H. J. C. (1996) J. Biomol. Struct. Dyn. **13**, 741–751
25   Bernstein, F. C., Koetzle, T. F., Williams, G. J. B., Meyer, E. F., Brice, M. D., Rodgers, J. R., Kennard, O., Shimanouchi, T. and Tasumi, M. (1977) J. Mol. Biol. **112**, 535–542
26   Zanotti, G., Ottonello, S., Berni, R. and Monaco, H. L. (1993) J. Mol. Biol. **230**, 613–624
27   Zanotti, G., Berni, R. and Monaco, H. L. (1993) J. Biol. Chem. **268**, 10728–10738
28   Cowan, S. W., Newcomer, M. E. and Jones, T. A. (1990) Proteins **8**, 44–61
29   Zanotti, G., Marcello, M., Malpeli, G., Folli, C., Sartori, G. and Berni, R. (1994) J. Biol. Chem. **269**, 29613–29620
30   Winter, N. S., Bratt, J. M. and Banaszak, L. J. (1993) J. Mol. Biol. **230**, 1247–1259
31   Kleywegt, G. J., Bergfors, T., Senn, H., Lemotte, P., Gsell, B., Shudo, K. and Jones, T. A. (1994) Structure **2**, 1241–1258
32   Kauzmann, W. (1959) Adv. Prot. Chem. **14**, 1–64
33   Eisenberg, D. and McLachlan, A. D. (1986) Nature (London) **319**, 199–203
34   Langlet, J., Pullman, B. and Berthod, H. (1970) J. Mol. Struct. **6**, 139–144
35   Poirier, R. A. and Yadav, A. (1989) Chem. Phys. Lett. **156**, 122–124
36   Beppu, Y. and Kakitani, T. (1990) Chem. Phys. **148**, 333–346
37   Aqvist, J., Sandblom, P., Jones, T. A., Newcomer, M. E., van Gunsteren, W. F. and Tapia, O. (1986) J. Mol. Biol. **192**, 593–604
38   Levitt, M., Sander, C. and Stern, P. S. (1985) J. Mol. Biol. **181**, 423–447
39   Ong, D. E. and Chytil, F. (1978) J. Biol. Chem. **253**, 828–832
40   Ong, D. E. (1984) J. Biol. Chem. **259**, 1476–1482
41   MacDonald, P. N. and Ong, D. E. (1987) J. Biol. Chem. **262**, 10550–10556
42   Levin, M. S., Locke, B., Yang, N. C., Li, E. and Gordon, J. I. (1988) J. Biol. Chem. **263**, 17715–17723
43   Braude, E. A., Jones, E. R. H., Koch, H. P., Richardson, R. W., Sondheimer, F. and Toogood, J. B. (1949) J. Chem. Soc. 1890–1897
44   Oroshnik, W., Karmas, G. and Mebane, A. D. (1952) J. Am. Chem. Soc. **74**, 295–304
45   Sivaprasadarao, A. and Findlay, J. B. C. (1994) Biochem. J. **300**, 437–442
46   Herr, F. M. and Ong, D. E. (1992) Biochemistry **31**, 6748–6755
47   Schreckenbach, T., Walckhoff, B. and Oesterhelt, D. (1977) Eur. J. Biochem. **76**, 499–511
48   Childs, R. F., Shaw, G. S. and Wasylishen, R. E. (1987) J. Am. Chem. Soc. **109**, 5362–5366
49   Honig, B., Dinur, U., Nakanishi, K., Balogh-Nair, V., Gawinowicz, M. A., Arnaboldi, M. and Motto, M. G. (1979) J. Am. Chem. Soc. **101**, 7084–7086
50   Nakanishi, K., Balogh-Nair, V., Arnaboldi, M., Tsujimoto, K. and Honig, B. (1980) J. Am. Chem. Soc. **102**, 7945–7947
51   Motto, M. G., Sheves, M., Tsujimoto, K., Balogh-Nair, V. and Nakanishi, K. (1980) J. Am. Chem. Soc. **102**, 7947–7949
52   Vijayakumar, E. K. S. and Balaram, P. (1984) Photochem. Photobiol. **39**, 667–672
53   Creuzet, F. C., McDermott, A., Gebhard, R., van der Hoef, K., Spijker-Assink, M. B., Herzfeld, J., Lugtenburg, J., Levitt, M. H. and Griffin, R. G. (1991) Science **251**, 783–786
54   DiNola, A., Roccatano, D. and Berendsen, H. J. C. (1994) Proteins **19**, 174–182